International Journal of Cast Metals Research

ISSN: 1364-0461 (Print) 1743-1336 (Online) Journal homepage: http://www.tandfonline.com/loi/ycmr20

Microstructure development during directional solidification of Sn–Ag–Cu ternary alloys

Osvaldo Fornaro & Carina Morando

To cite this article: Osvaldo Fornaro & Carina Morando (2017): Microstructure development during directional solidification of Sn–Ag–Cu ternary alloys, International Journal of Cast Metals Research, DOI: 10.1080/13640461.2017.1379261

To link to this article: http://dx.doi.org/10.1080/13640461.2017.1379261

INTERNATIONAL JOURNAL OF CAST METALS RESEARCH, 2017
https://doi.org/10.1080/13640461.2017.1379261

Taylor & Francis
Taylor & Francis Group

Microstructure development during directional solidification of Sn–Ag–Cu ternary alloys

Osvaldo Fornaro[a,b] and Carina Morando[a,b]

[a]Instituto de Física de Materiales Tandil — IFIMAT, Tandil, Argentina; [b]Centro de Investigaciones en Física e Ingeniería del Centro de la Provincia de Buenos Aires — CIFICEN, Universidad Nacional del Centro de la Provincia de Buenos Aires (UNCPBA — CICPBA — CONICET), Tandil, Argentina

ABSTRACT

Replace of Pb–Sn with Pb-free solders (LFS) is one of the most important issues in the electronic industry. Eutectic and near-eutectic Sn–Ag–Cu (SAC) alloys are recommended as lead-free replacement in welding processes of electronic devices. Close to the eutectic ternary composition, the solidification occurs with three distinctive phases: Sn-rich dendritic primary phase, and the intermetallic phases Ag_3Sn and Cu_6Sn_5, showing a limited solubility into the Sn-rich phase. Given the key role of the solidification process in the microstructure development of the alloy, samples of Sn–Ag–Cu with a composition close to the ternary eutectic were directionally grown to analyze the mechanisms involved in the solidification process of these alloys. The typical microstructure agrees withe above description, but shows two different mechanisms, depending on the interface advance velocity, resulting in different distribution of the intermetallic phases.

ARTICLE HISTORY
Received 19 September 2016
Accepted 8 September 2017

KEYWORDS
Directional solidification; Eutectic alloys; lead-free solder alloys (LFS); solidification structures

1. Introduction

Ternary eutectic Sn–Ag–Cu have received particular attention because this system is a main candidate to be a lead-free solder (LFS) alloy replacement of traditionally used Sn–Pb eutectic. Microstructural characteristics are reported as containing an homogeneous primary phase coupled with binary eutectics [1]. The extent of primary phase affects the mechanical properties, mainly under moderate and high working temperatures. Previous studies of binary and ternary eutectics are based on the fundamental works of Jackson and Hunt [2] and McCartney et al. [3,4]. According to these models or descriptions, a microstructure of columnar cells and lamellar secondary phases in the middle of an homogenous primary phase is expected.

The Sn–Ag–Cu ternary eutectic shows this type of microstructure, with an homogeneous primary phase of Sn with small quantities of Ag and Cu in solution and the intermetallic phases Cu_6Sn_5 (η) and Ag_3Sn (ϵ). It is expected that the solidification of a ternary alloys would be more complex than the solidification of a binary alloy. Being a ternary alloy, there are more diffusion paths between species, both during the cooling and solidification as in the alloy working life at high temperature. Also, whilst Sn–Pb is formed by two non-faceted phases, the ternary Sn–Ag–Cu alloys are formed by two faceted phases into a non-faceted matrix, which means that the growth could be more influenced by crystallographic effects [5].

Process parameters that affect the resultant microstructure during the soldering process are under active study. The interest include the reactive wetting due to the formation of η phase when the Cu substrate is in contact with the liquid bath [6–10] and the solid state transformation from hexagonal η at temperatures above 459 K to monoclinic η' below that temperature during the freezing of the alloy [11–14]. This transformation also could to appear during the solder joints lifetime [11]. In this sense, directional solidification is a useful tool that allowed us to control the process variables such as advance velocity and thermal gradient in front of the interface and let us to study the microstructure development as a function of the process parameters [15,16].

The aim of this work is to perform directional growth of Sn–Ag–Cu ternary eutectics to study the formation of microstructures during the solidification of these alloys to eventually apply these results to the development of soldering process.

2. Experimental

The alloys were prepared starting from 99.99% analytical purity elements melted in an electrical furnace under a protective Ar atmosphere. Pre-ingots were poured into a 10 mm internal diameter by 120 long cylinders. First, the binary eutectics Sn-0.9 wt-%Cu and Sn-3.5 wt-%Ag alloys were obtained and used as mother alloys

CONTACT Osvaldo Fornaro ofornaro@exa.unicen.edu.ar

[17,18]. The chemical composition of the samples was Sn-3.5 wt-%Ag-0.9 wt-%Cu, and was obtained by the addition of Ag and Cu to the previously obtained binary eutectics, and poured in a similar way. These ingots were located into quartz tubes of 8 mm internal diameter, to be directionally grown.

The eutectic composition could be observed in the intersection of the monovariant lines of the phase diagram shown in Figure 1. Such diagram was calculate using a thermodynamic calculation software[1] and the associate databases for lead-free alloys [19–25]. As can be extracted by calculus, the theoretical eutectic composition of the ternary alloy is Sn-8.5 wt-%Ag-3.75 wt-%Cu, corresponding to a transformation temperature of 489,08 K. Also, the expected solidification path and phases distribution as a function of temperature for the composition used in this work can be seen in Figure 2. As the composition of the sample is close to the ternary eutectic composition, the solidification is almost isothermal, although a small amount of primary phase $\beta\,(\mathrm{Sn})$ appears at the solidification starts. After the monovariant binary eutectic reaction

$$L \rightarrow (\beta + \eta) \tag{1}$$

the ternary invariant reaction

$$L \rightarrow \beta + \eta + \epsilon \tag{2}$$

take place at the temperature $T_E = 489$ K. Once all the sample has solidified, the phase fraction expected under equilibrium conditions for $\beta\,(\mathrm{Sn})$, $\eta\,(\mathrm{Cu_6Sn_5})$ and $\epsilon\,(\mathrm{Ag_3Sn})$ is condensed in Table 1.

Directional growth was performed in a Bridgman like apparatus, as has been previously reported [15, 16]. The device consists of two chambers located in a cylindrical symmetry. Upper chamber consists of an alumina core with a heating coil with electronic temperature control. The lower section is refrigerated by water circulation. This disposition allows us to obtain a fixed thermal gradient in the place where the samples were located to be directionally grown. The pulling system of the samples was based in a stepper motor and a gear box, which permitted a translation velocity in the 0–10 $\mu\mathrm{ms}^{-1}$ range. The displacement velocity was measured and controlled with a linear variable differential transformer (LVDT) and a signal conditioning interface. The data was sent to a personal computer, which drives the motor. This scheme provides a very precise motion, resulting with a precision of $\pm 0.1\ \mu\mathrm{ms}^{-1}$.

The temperatures in the sample were taken using a double K-type (CrNi-AlNi) thermocouple, which allows us to determine temperature and thermal gradient simultaneously. Measuring was made by an Acquisition Datalogger system, with an experimental error of ± 0.5 K. In this work, we fixed the thermal gradient in each set of experiences, which let us to take the velocity as the control parameter of the problem.

The preparation of the surface for optical microstructural observation and analysis requires particular attention, because this alloy can show plastic deformation during the mechanical polishing giving place to twinning formation and the re-precipitation of small grains on the surface. To avoid these effects, an extremely slow and continuously refrigerated mechanical polishing was made. The microstructure was observed both in longitudinal (respect to the growth direction) and cross sections views. The surface was set up by mechanical polishing with up to 1000 grit SiC abrasive paper lubricated with water and then with 6 and 3 μm diamond powder refrigerated with alcohol. In some opportunities, chemical polishing and electrolytic polishing were also used. Electro-polish also generates a thick oxidized surface, which allows us to detect changes in crystallographic orientation when it is observed under polarized light. The samples were observed using optical microscopy under bright field, polarized light and differential interferometry contrast conditions. While different grains were observed with slight lighting changes, the grain boundaries were not revealed [18,26].

3. Results and discussion

Directionally growth experiences were carried out under velocities of 0.5; 1; 2 and 5 $\mu\mathrm{ms}^{-1}$ and thermal gradient of $G_L = 2.5\ \mathrm{Kmm}^{-1}$. The growths were developed through all length of the sample, that is approximately 100 mm long. However some experiences were quenched in order to allow the observation of the microstructure at the interface during the crystal growth and to verify the growth directionality [16]. Figure 3 shows a directional growth of the ternary Sn-3.5 wt-%Ag-0.9 wt-%Cu as-quenched. The morphology in this case was dendritic, showing a primary spacing of approximately $\lambda_1 = 100\,\mu$m. In the bottom part of the picture the crystal grown upward is observed, whilst in the superior part the quenched liquid can be seen.

In this case the microstructure is formed has been mentioned before, by a primary homogeneous dendritic phase, composed by Sn, Ag and Cu in solution, and the intermetallic phase $\mathrm{Ag_3Sn}$ forming small precipitates and $\mathrm{Cu_6Sn_5}$ in a needle geometry. As can be seen in Figure 2, the composition of our samples are close the eutectic composition, in such a way that these three phases appears almost at the same temperature of 489 K.

However the structure does not show a dendritic pattern for velocities smallest than $V = 0.5\ \mu\mathrm{ms}^{-1}$ for the thermal gradient of $G_L = 2.5\ \mathrm{Kmm}^{-1}$ used in this work. In these cases, the resultant microstructure consist of cellular $\beta\,(\mathrm{Sn})$, where the inter-cellular space is occupied by needles of $\eta\,(\mathrm{Cu_6Sn_5})$. Also small precipitates

[1] ThermoCalc software USLD1 database for solder alloys.

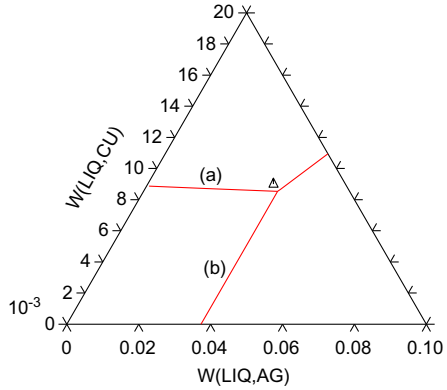

Figure 1. Monovariant lines in the ternary phase diagram of Sn–Ag–Cu system. Triangle indicates the alloy composition used in this work. (a) indicate the monovariant binary eutectic transformations $L \rightarrow \beta + \eta$ and (b) $L \rightarrow \beta + \epsilon$ respectively. The intersection indicate the univariant $L \rightarrow \beta + \eta + \epsilon$ ternary eutectic reaction.

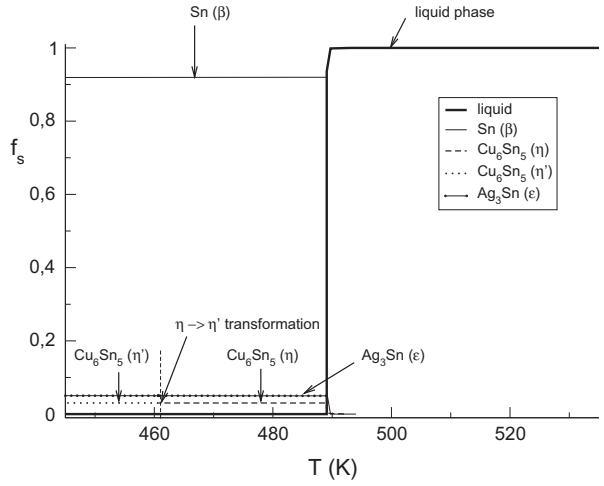

Figure 2. Solidification path for the alloy used in present work. The liquid transforms to β, η and ϵ phases at 489.07 K. After that, it can be seen the solid–solid transformation $\eta \rightarrow \eta'$ at 460.69 K.

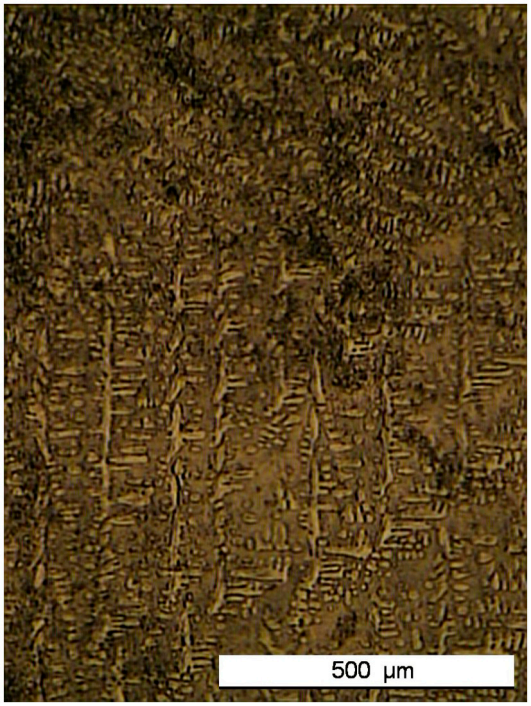

Figure 3. Macrography of a solid–liquid quenched interface, $V = 1\ \mu\text{ms}^{-1}$, $G_L = 2.5\ \text{Kmm}^{-1}$.

of intermetallic ϵ (Ag_3Sn) appears homogeneously distributed into the matrix, as can be seen in the Figure 4(a). Also it can be seen that the alignment of the η fibers gradually change, forming a structure similar to a secondary distribution, starting from a main fiber. In this way, the spacing of the cellular array is defined by the separation of these main fibers, which seems to be independent of the secondary fibers spacing or distribution.

The Cu_6Sn_5 spacing does not seem to be related to the velocity, at least in this range of advance velocities. This phase seem to be locate in the inter-space between the Ag_3Sn phase, without an evident order, as can be seen with a greater detail in Figure 4(b). This is against to the reported behavior of the binary Sn-0.9 wt-%Cu eutectic directionally grown, for which the Cu_6Sn_5 phase distribution shows a well determined spacing [27].

At greater velocities, the typical microstructure result similar to a bi-phase dendritic growth morphology formed by an homogeneous primary phase of Sn–Cu–Ag in solution and the interdendritic zone which is formed by three phases: the matrix and the other two intermetallic phases mentioned before. Figure 5(a) shows a longitudinal section grown at $V = 2\ \mu\text{ms}^{-1}$ and $G_L = 2.5\ \text{Kmm}^{-1}$. The interdendritic zone can be seen in a more detailed view at Figure 5(b). It can be noticed that in this interdenditic zone the microstructure is thinner than cellular growth. A similar behavior can be seen at $V = 5\ \mu\text{ms}^{-1}$ and $G_L = 2.5\ \text{Kmm}^{-1}$, as shown at Figure 6.

Under the frame of this experiences, for velocities greater than $1\ \mu\text{ms}^{-1}$, the growth is developed as a coupled eutectic growth, where the primary phase is an homogeneous dendritic rich Sn phase with Ag and Cu in solution, that could be growing as non-faceted, while the other two present phases grow as faceted, in the interdendritic spacing. The precipitation of intermetallic Ag_3Sn and Cu_6Sn_5 is well differentiated. At greater velocity the growth morphology changes dramatically, showing a bi-phase dendritic growth behaviour, with a primary homogeneous phase and an interdendritic zone that contains the three phases of the ternary eutectic. This behaviour could be possible by the high undercooling of the primary Sn-rich phase, which was observed in cooling curves and calorimetric experiments [17]. This undercooling let the change from a cellular

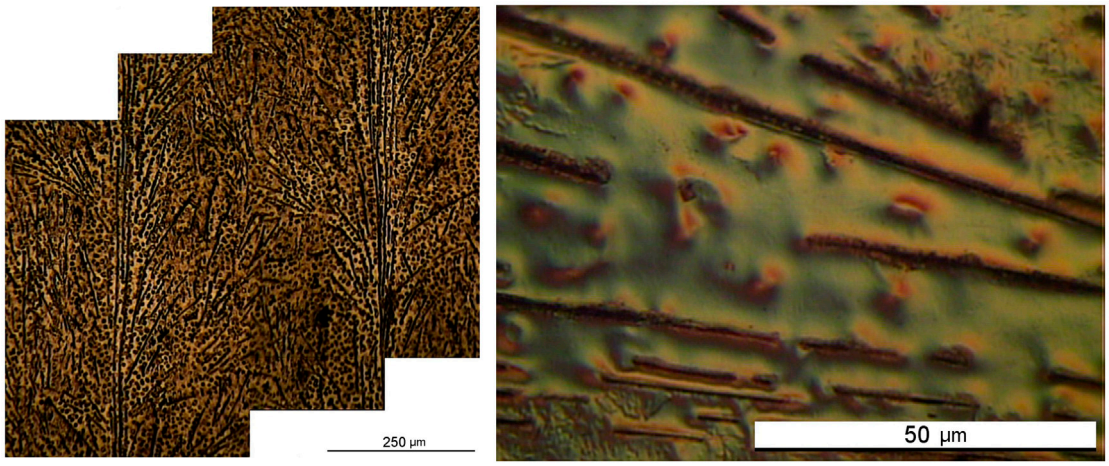

Figure 4. Directional growth of Sn-3.5 wt-%Ag-0.9 wt-%Cu, grown at $V = 0.5\,\mu\text{ms}^{-1}$, $G_L = 2.5$ Kmm^{-1}. (a) longitudinal view, (b) detailed view of present phases.

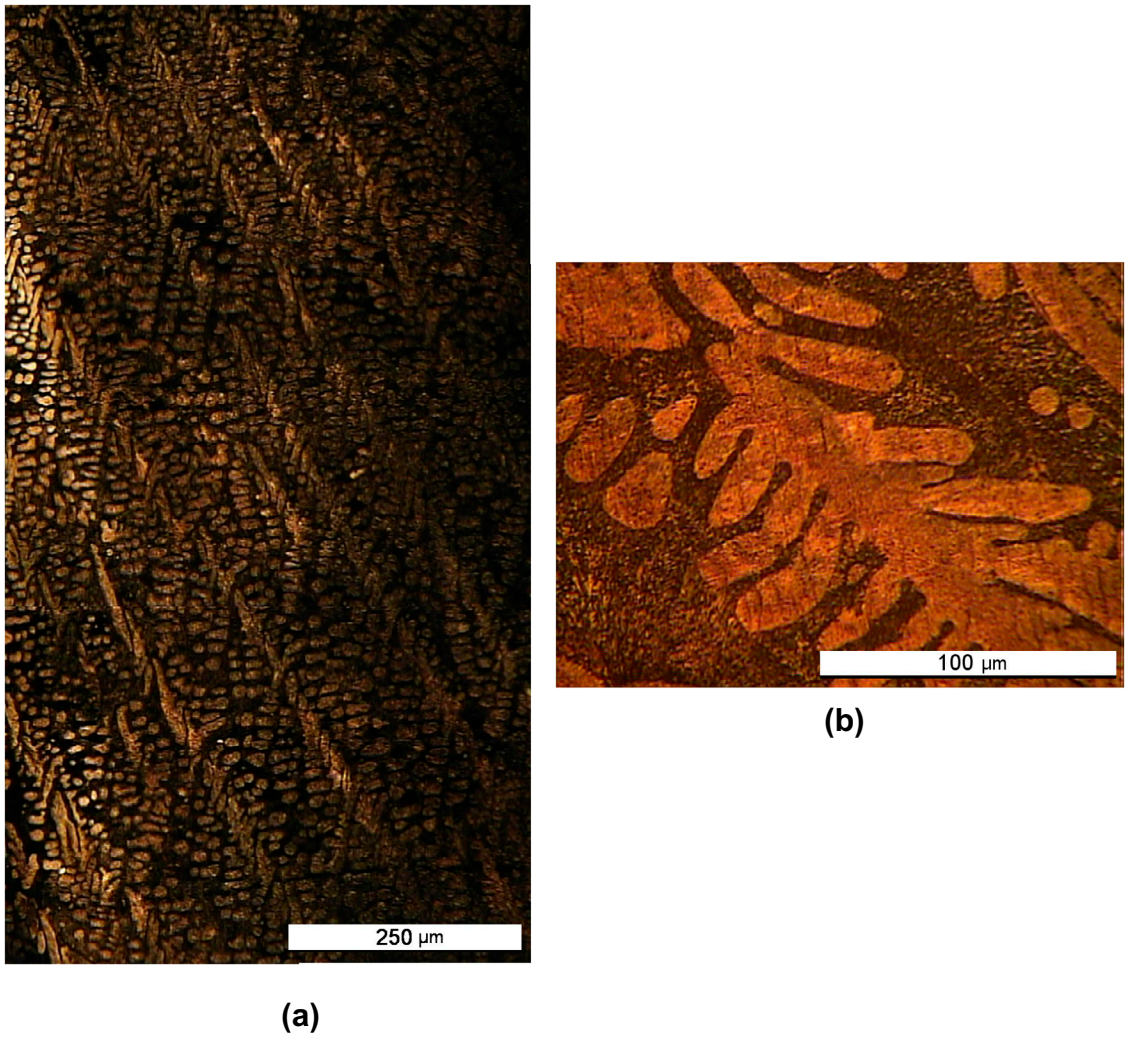

Figure 5. Directional growth of Sn-3.5 wt-%Ag-0.9 wt-%Cu under the conditions a) $V = 2\,\mu\text{ms}^{-1}$, $G_L = 2.5$ Kmm^{-1}, (a) longitudinal view, growth direction is upward; (b) detailed view of the dendritic growth.

Table 1. Expected phase fractions after solidification of Sn-3.5 wt-%Ag-0.9 wt-%Cu calculated under equilibrium conditions.

	β (Sn)	η (Cu_6Sn_5)	ϵ (Ag_3Sn)
phase fraction	0.92	0.03	0.05

pattern to a dendritic one, even for chemical concentrations close to the eutectic used in this work.

3.1. Interfiber spacing

Due to the limited diffusion of β and η phases, a wide coupled eutectic zone can be expected. In this way, the Jackson–Hunt eutectic theory could be used as a starting point to interpret the obtained microstructures [2,28,29]. In principle, this theory is useful for regular non-faceted/non-faceted eutectics, which is not this case. However, it can be useful interpret the behavior of faceted/non-faceted eutectics, provided some constants of the model could to be adapted. Under the supposition of a minimum undercooling, the relation between the average undercooling in front of the isothermal interface (ΔT), the advance interface velocity (V) and the spacing of the fibers is

$$\Delta T = K_1 V \lambda + \frac{K_2}{\lambda} \tag{3}$$

where K_1 and K_2 are constants that depends on the alloy and could be found in literature [30]. Using the condition of minimum undercooling, a relation between the spacing and the interface advance velocity can be found

$$\lambda = K' V^{-1/2} \tag{4}$$

which in principle could be used in the prediction of the fiber primary phase spacing. In the Equation (4), $K' = \sqrt{K_2/K_1}$.

In Figure 7 the primary spacing λ_1 is plotted against the interface advance velocity V. The closed squares are used to show a dendritic primary β (Sn) phase. The cellular morphology is obtained for the lower velocity, allowing a different distribution of the intermetallic phases. The primary spacing of the cellular growth is also added to the graph as an open square symbol. It can be seen that the dendritic stage follows a power approximation, which can be fitted with

$$\lambda_1 = 200.432 \cdot V^{-0.427} \tag{5}$$

where λ_1 is measured in (μm) and the velocity V in (μms^{-1}). The power law (5) does not exactly corresponds to the value shown in the Equation (4) of $(V^{-1/2})$, which should not be surprising due to the original analysis is valid for non faceted-non faceted dilute alloys, which clearly is not this situation [29].

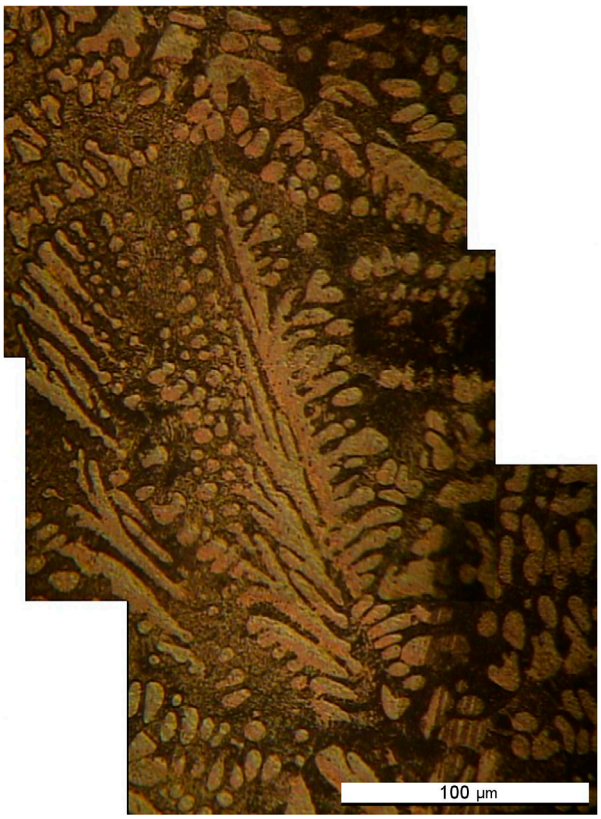

Figure 6. Directional growth of Sn-3.5 wt-%Ag-0.9 wt-%Cu under $V = 5\,\mu ms^{-1}$ and $G_L = 2.5$ Kmm^{-1}. Growth direction is upward.

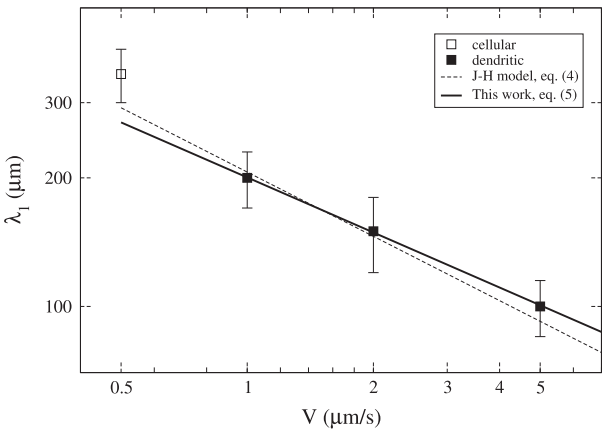

Figure 7. Primary spacing behavior plotted against the advance velocity at fixed thermal gradient of $G_L = 2.5$ Kmm^{-1}.

The results partially agrees with the previously reported by Schaeffer and Lewis [5], whom obtained a similar change of behavior in the growth mechanism similar to the reported in this work, for a interface velocity close to $0.826\,\mu ms^{-1}$ but for a greater thermal gradient value of 7.5 Kmm^{-1}. Anyway, a range of velocities where both mechanisms could coexist would be expected to exist. More evidence of the distribution of

the intermetallic phases in the cellular stage would be needed.

4. Conclusions

Directional growth of Sn-3.5 wt-%Ag-0.9 wt-%Cu ternary samples were developed in the range of advance velocities of the interface of 0.5; 1; 2 and 5 μms^{-1}. All experiences were developed at the same thermal gradient of $G_L = 2.5\,Kmm^{-1}$. It was found that there are at least two mechanisms of growth that could be identified. At low speed, formally below $V = 1\,\mu ms^{-1}$, the growth is formed by a homogeneous primary phase rich in Sn with Ag and Cu in solution, whereas Cu_6Sn_5 and Ag_3Sn intermetallic phases are distributed in the resultant crystal. The first one is aimed partly allowing the growth direction define a cell type spacing, but also distributed in the form of needles away from this main fiber. Ag_3Sn phase appears homogeneously distributed in the form of small precipitates. At higher speeds, the growth is characterized by a dendritic growth of Sn primary phase, with the interdendritic spacing formed by the two above-mentioned intermetallic phases distributed homogeneously into the interdendritic spacing. The primary spacing follows a decreasing power law, close to the prediction of the Jackson–Hunt model of eutectic growth for fibrous eutectic systems.

Disclosure statement

No potential conflict of interest was reported by the authors.

Funding

This work was carried out at IFIMAT and CIFICEN and has been partially supported by ANPCyT (Agencia Nacional de Promoción Científica y Tecnológica), CONICET (Consejo Nacional de Investigaciones Científicas y Técnicas), SeCAT-UNCPBA (Secretaría de Ciencia, Arte y Tecnología de la Universidad Nacional del Centro de la Provincia de Buenos Aires) and CICPBA (Comisión de Investigaciones Científicas de la Provincia de Buenos Aires).

ORCID

Osvaldo Fornaro http://orcid.org/0000-0003-1150-8531

References

[1] Kurz W, Fisher DJ. Dendrite growth in eutectic alloys: the coupled zone. Int Met Rev. 1979;24:177–204.
[2] Jackson KA, Hunt JD. Lamellar and rod eutectic growth. Trans Metall Soc AIME. 1966;236:1129–1142.
[3] McCartney DG, Hunt JD, Jordan RM. The structures expected in a simple ternary eutectic system: part 1. theory. Metall Trans A. 1980;11:1243–1249.
[4] McCartney DG, Jordan RM, Hunt JD. The structures expected in a simple ternary eutectic system: part II. the Al-Ag-Cu ternary system. Metall Trans A. 1980;11:1251–1257.
[5] Schaefer R, Lewis D. Directional solidification in a AgCuSn eutectic alloy. Metall Mater Trans A. 2005;36:2775–2783. DOI:10.1007/s11661-005-0273-2
[6] Villanueva W, Grönhagen K, Amberg GJ. Ågren. Multicomponent and multiphase modeling and simulation of reactive wetting. Phys Rev E. 2008;77:056313.
[7] Villanueva W, Boettinger W, McFadden G, et al. A multicomponent and multiphase model of reactive wetting. In: 7th International Conference on Multiphase Flow, ICMF; 2010 May 30–Jun 4; Tampa, FL; 2010.
[8] Sobczak N, Kudyba A, Nowak R, Radziwill W, et al. Factors affecting wettability and bond strength of solder joint couples. Pure Appl Chem. 2007;79:1755–1769. *Paper based on a presentation at the 12th International IUPAC Conference on High Temperature Materials Chemistry (HTMCXII), 2006 Sept 18–22, Vienna, Austria.
[9] Amore S, Ricci E, Borzone G, Novakovic R. Wetting behaviour of lead-free sn-based alloys on Cu and Ni substrates. Mater Sci Eng A. 2008;495:108–112. Fifth International Conference on High Temperature Capillarity HTC-2007, Alicante, Spain.
[10] Matsumoto T, Nogi K. Wetting in soldering and microelectronics. Ann Rev Mater Res. 2008;38:251–273.
[11] Feng G, Hiroshi N, Tadashi T. Microstructure characterization of Cu6Sn5-based intermetallic compounds at solder matrix and relevant solder joints. Trans JWRI. 2005;34:57–61. Transactions of JWRI is published by Joining and Welding Research Institute, Osaka University, Ibaraki, Osaka, Japan.
[12] Laurila T, Vuorinen V, Kivilahti J. Interfacial reactions between lead-free solders and common base materials. Mater Sci Eng R Rep. 2005;49:1–60.
[13] Nogita K, Gourlay C, McDonald S, et al. Kinetics of the $\nu-\nu'$ transformation in Cu_6Sn_5. Scr Mater. 2011;65:922–925.
[14] Zeng G, McDonald SD, Read JJ, et al. Kinetics of the polymorphic phase transformation of Cu_6Sn_5. Acta Mater. 2014;69:135–148.
[15] Fornaro O, Palacio HA, Biloni H. Segregation substructures in dilute Al-Cu alloys directionally solidified. Mater Sci Eng A. 2006;417:134–142.
[16] Ochoa H, Fornaro O, Bustos O, et al. Directional solidification of dilute Sn-Pb alloys. Int J Cast Met Res. 2012;25:201–206.
[17] Morando CN, Fornaro O, Garbellini OB, et al. Thermal properties of Sn-based solder alloys. J Mater Sci Mater Electron. 2014;25:3440–3447.
[18] Morando C, Fornaro O, Garbellini O, et al. Fluidity of Sn-based eutectic solder alloys. J Mater Sci Mater Electron. 2015;26:9478–9483.
[19] Dinsdale A. SGTE data for pure elements. Calphad. 1991;15:317–425.
[20] Hayes FH, Lukas HL, Effenberg G, et al. Ag-Cu, Ag-Pb, Ag-Cu-Pb. Z. Metallkd. 1986;77:749–754.
[21] Shim J, Oh C, Lee B, Lee D. Thermodynamic assessment of the Cu-Sn system. Z. Metallkd. 1996;87:205–212.
[22] Oh C-S, Shim J-H, Lee B-J, et al. A thermodynamic study on the Ag-Sb-Sn system. J Alloys Compd. 1996;238:155–166.
[23] Moon K, Boettinger W, Kattner U, et al. Experimental and thermodynamic assessment of Sn-Ag-Cu solder alloys. J Electron Mat. 2000;29:1122–1136.
[24] Moon K-W, Boettinger W. Accurately determining eutectic compositions: the Sn-Ag-Cu ternary eutectic. JOM. 2004;56:22–27.

[25] Kattner U. Phase diagrams for lead-free solder alloys. JOM. 2002;54:45–51.
[26] Castro ML, Fornaro O. Optical microscopy in the study of metallic alloys. Acta Microsc. 2010;19:94–99.
[27] Grugel R, Brush L. Evaluation of the rodlike Cu6Sn5 phase in directionally solidified tin 0.9 wt-pct copper eutectic alloys. Mater Charact. 1997;38:211–216.
[28] Hunt JD, Jackson KA. Binary eutectic solidification. Trans Metall Soc AIME. 1966;236:843–852.
[29] Dantzig J, Rappaz M. Solidification. Materials. Italy: EPFL Press; 2009.
[30] Çadırlı E, Böyük U, Engin S, et al. Investigation of the effect of solidification processing parameters on the rod spacings and variation of microhardness with the rod spacing in the Sn-Cu hypereutectic alloy. J Mater Sci Mater Electron. 2010;21:608–618.